X-RAY SCATTERING OF VESICLES OF *N*-ACYL SPHINGOMYELINS

Determination of Bilayer Thickness

P. R. MAULIK, D. ATKINSON, and G. G. SHIPLEY
Biophysics Institute, Departments of Biochemistry and Medicine, Boston University School of Medicine, Housman Medical Research Center, Boston, Massachusetts 02118

ABSTRACT A series of *N*-acyl sphingomyelins (C16:0, C18:0, C20:0, C22:0, and C24:0) have been synthesized and single bilayer vesicles formed by sonication and ultracentrifugation. X-ray scattering data have been collected from the sphingomyelin vesicles at 50°C in the melted-chain state. The x-ray scattering data have been transformed to the corresponding Patterson functions and Fourier electron density profiles; analysis of these functions has provided the intrabilayer phosphate-phosphate separation d_{p-p}, a measure of the lipid bilayer thickness. The bilayer thickness increases linearly with increasing chain length (increment 1.3–1.4 Å) and the intercept, 14.3–15.0 Å, suggests a contribution of 7.0–7.5 Å for each phosphorylcholine group to the bilayer thickness. The electron-density profiles have features suggestive of chain interdigitation when the length of the *N*-acyl chain (C20:0, C22:0, and C24:0) exceeds significantly the length of the invariant sphingosine chain.

INTRODUCTION

The basic structural motif of the lipid compartment of cell membranes is the lipid bilayer, characterized by a distinct hydrophobic central domain contributed by acyl chains bounded by two polar interfacial regions defined by lipid polar groups. The structure and properties of many glycerol-based phospholipids have been determined and the importance of the melted-chain L_α state of phospholipids for membrane function has been emphasized. A critical parameter to determine is the lipid bilayer thickness; by using x-ray and neutron diffraction methods, many such determinations have been made for such phospholipids as phosphatidylcholine (PC), phosphatidylethanolamine, phosphatidylserine, etc. These studies have been conducted on phospholipid crystals, oriented multibilayers at low hydration, and unoriented multibilayers at high hydration and a detailed understanding of bilayer thickness in gel and liquid crystal multibilayer states has resulted. Much less information on bilayer structural parameters is available for single bilayer systems. Early studies showed that single bilayer systems of PC produced by sonication were suitable for study by diffraction methods (1–3) and the studies of Wilkins et al. (1) provided the first measurements of lipid bilayer thickness in single bilayer systems. Recently, Lewis and Engelman (4) have used a similar x-ray scattering approach to define the bilayer thickness of two series of saturated and mono-unsaturated PCs. In a related study (5), these authors have shown that the bilayer thickness can influence the in-plane organization of a membrane spanning protein, bacteriorhodopsin.

Our own interests have been focused recently on the structure and properties of the sphingosine-based sphingomyelins (SM) and glycosphingolipids (6–8). For SM, we have synthesized a series of *N*-acyl SM in which the acyl chain is varied from C16:0 to C24:0 (9). In this study, we report measurements of bilayer thickness as a function of *N*-acyl chain length for single bilayers of SM produced by sonication.

MATERIALS AND METHODS

Materials

C16:0, C18:0, C20:0, C22:0, and C24:0 SM were synthesized from bovine brain SM (Calbiochem-Behring Diagnostic, San Diego, CA) following acid hydrolysis deacylation to sphingosylphosporylcholine (SPC), followed by reacylation of SPC using fatty acyl imidazoles (for details, see reference 9). The samples were shown to be chemically pure (>99%) using thin-layer chromatography, solvent system chloroform/methanol/water/acetic acid (65:25:4:1, vol/vol), and high performance liquid chromatography (9).

Preparation of Single Bilayer Vesicles of *N*-Acyl SM

Single bilayer vesicles of SM were prepared by sonication according to the method described by Barenholz et al. (10). 75 mg of individual *N*-acyl SM were suspended in 1.5 ml of doubly distilled, deionized water. The samples were sonicated under nitrogen at 50°C using a Branson sonifier equipped with a microtip. Sonication was performed at power level 3 in a pulsing mode with a 30% duty cycle until the solutions were clear. The total sonication time was for 45 min to 1 h. After sonication, the solutions were centrifuged in a Beckman Model L8-70 ultracentrifuge (40.3 rotor [Beckman Instruments, Inc., Palo Alto, CA]) at 35,000 rpm at 50°C to sediment titanium fragments, large inhomogeneous vesicles, and any

residual multibilayer vesicles. The supernatants containing homogeneous, single bilayer vesicles of *N*-acyl SM were transferred immediately into 1 mm (i.d.) quartz capillaries for x-ray scattering experiments and, at the same time, into small plastic vials for lipid analysis. Lipid concentrations were determined using a modified assay for phosphorus as described by Bartlett (11).

X-Ray Small Angle Scattering

X-ray scattering data from sonicated, single bilayer vesicles of *N*-acyl SM were recorded using a Jarrell-Ash microfocus x-ray generator and a slit collimated Luzzati-Baro camera modified to include a single mirror focusing system. Scattered intensities were recorded as a function of scattering angle, 2θ, using a linear position-sensitive detector (Tennelec Inc., Oak Ridge, TN) coupled to a computer-based analysis system (Tracor Northern, WI). After being sealed, quartz capillaries containing *N*-acyl SM vesicles were placed in a variable temperature sample holder and x-ray scattering data collected at 50 ± 0.5°C. Nickel-filtered CuK_α radiation was used and the sample to detector distance was 339–343 mm. X-ray scattering data corresponding to an angular range s ($= 2 \sin\theta/\lambda$) of 0.0015–0.1245 $Å^{-1}$ were recorded for all *N*-acyl SM samples. For each *N*-acyl SM sample, x-ray scattering data were recorded from the empty capillary tube and the capillary tube containing solvent (in this case, water). In addition, the intensity of the primary beam in the absence and presence of capillary tube and sample were recorded for intensity scaling purposes.

The x-ray scattering data for each SM sample were scaled and buffer-subtracted in the following way: (*a*) The primary beam was attenuated with three nickel filters and the beamstop removed. The direct, primary x-ray was recorded with (*i*) no tube or sample (A_E), (*ii*) empty tube (A_T), (*iii*) tube filled with buffer (A_B), and (*iv*) tube filled with sample (A_S). (*b*) The beamstop and a single nickel filter were replaced and the x-ray scattering data were recorded for (*i*) empty tube ($I_T[s]$), (*ii*) tube filled with buffer ($I_B[s]$), and (*iii*) tube filled with sample ($I_S[s]$). The scattering data were placed on an absolute scale and buffer-subtracted according to the following equation (for data correction procedures, see references 12 and 13):

$$I(s) = \left(I_S \cdot \frac{A_E}{A_S} - I_T \cdot \frac{A_E}{A_T}\right) - \delta\left(I_B \cdot \frac{A_E}{A_B} - I_T \cdot \frac{A_E}{A_T}\right), \quad (1)$$

where δ represents the volume fraction of buffer, calculated as $\delta = 1 - c/1000\,\bar{v}$, where c is the concentration of SM (mg/ml) and $\bar{v}$ the specific volume of SM (assumed to be 1.014 ml/g).

The geometry of the x-ray scattering camera used in these studies results in a slit height weighting function <5 mm half length. With this geometry, slit-smearing effects are confined to the very small angle region of the data ($s < 1/150$ $Å^{-1}$). The small contribution of this region of the data to the Fourier transform of either the scattered intensity or amplitude is minimized further by the Lorentz correction (s^2) to give the scattering of the bilayer cross section.

RESULTS

X-Ray Scattering from C16:0-SM Vesicles

The uncorrected x-ray scattering data for C16:0-SM vesicles (concentration 39.4 mg/ml) at 50°C recorded over the angular range $s = 0.001 - 0.070$ $Å^{-1}$ are shown in Fig. 1 *a*. The data acquisition time was 20.7 h. A strong maximum is evident at $s = 0.015$ $Å^{-1}$, with a weaker maximum at $s = 0.055$ $Å^{-1}$. Following scaling and buffer subtraction according to Eq. 1, the scattering curve shown in Fig. 1 *b* is obtained with a clearer definition of the second maximum. A plot of $I(s)*s^3$ as a function of s^3 (Fig. 1 *c*) shows that the outer part of the scattering curve follows Porod's law (for an application to lipid bilayers, see reference 14). The slope of the Porod plot gives a constant $K2$ that arises from short-range electron-density fluctuations; this constant was subtracted from the experimental data. Finally, the data were corrected for Lorentz and polarization factors and the final smoothed, scattering curve from the C16:0-SM bilayer is shown in Fig. 1 *d*. Two well defined maxima at $s = 0.025$ and 0.055 $Å^{-1}$ are present.

The corrected scattering curve shown in Fig. 1 *d* is analyzed in two ways to provide a measure of the bilayer thickness of C16:0-SM vesicles. First, the scattering data can be transformed directly to the corresponding Patterson function according to

$$P(X) = \frac{1}{\pi}\int I(s) \cdot s^2 \cos(2\pi sX)\, ds. \quad (2)$$

Fig. 2 *a* shows the bilayer Patterson function where the first non-origin peak (arrowed) represents the vector distance between the two electron-dense phosphate groups of the phosphorylcholine polar groups of SM located on the two surfaces of the bilayer. This provides a measure of the lipid thickness, d_{p-p}, and for C16:0-SM a value of 36.5 Å is obtained. The large origin peak arises from the addition of all zero-length vectors.

Second, making assumptions about the centrosymmetric nature of lipid bilayers,[1] a plot of the scattering amplitude $F(s)$ ($= \sqrt{I[s]}$) locates the s values at which the amplitude curve changes sign. Following phase assignment, the electron-density distribution across the SM bilayer is calculated according to

$$\rho(X) = \frac{1}{A}\int_0^\infty s\sqrt{I(s)} \cdot \cos(2\pi sX)\, ds. \quad (3)$$

The electron-density profile across the C16:0-SM bilayer is shown in Fig. 2 *b*. This profile is typical of lipid bilayers, showing a trough at $X = 0$ Å corresponding to the bilayer center and two peaks at ±18.0 Å due to the electron-rich phosphate groups.

Thus, a bilayer thickness, $d_{p-p} = 36.0$ Å is found by this method, as expected, in good agreement with that derived

[1] A reviewer raises an interesting point about possible curvature effects on the bilayer parameters measured. We have not determined whether *N*-acyl chain length influences in any way the size of the SM vesicles formed. Our primary objective was to produce single bilayer vesicles, thus removing interbilayer scattering effects. However, (*a*) based on analogy with sonicated PC systems, all of the SM vesicles produced by prolonged sonication and further fractionated by ultracentrifugation are probably small (<500 Å); (*b*) at the resolution of these studies the assumption of centrosymmetry is certainly valid for all members of the SM series; (*c*) based on the data collected so far, we are not able to evaluate possible contributions of bilayer curvature to thickness (nor, as far as we are aware, is anybody else for similar systems); and finally, (*d*) we have made vesicles of di C16:0-PC by the sonication/ultracentrifugation method, analyzed the bilayer thickness by x-ray scattering (as for the SM series), and find an identical bilayer thickness, 37 Å, to that reported by Lewis and Engelman (4).

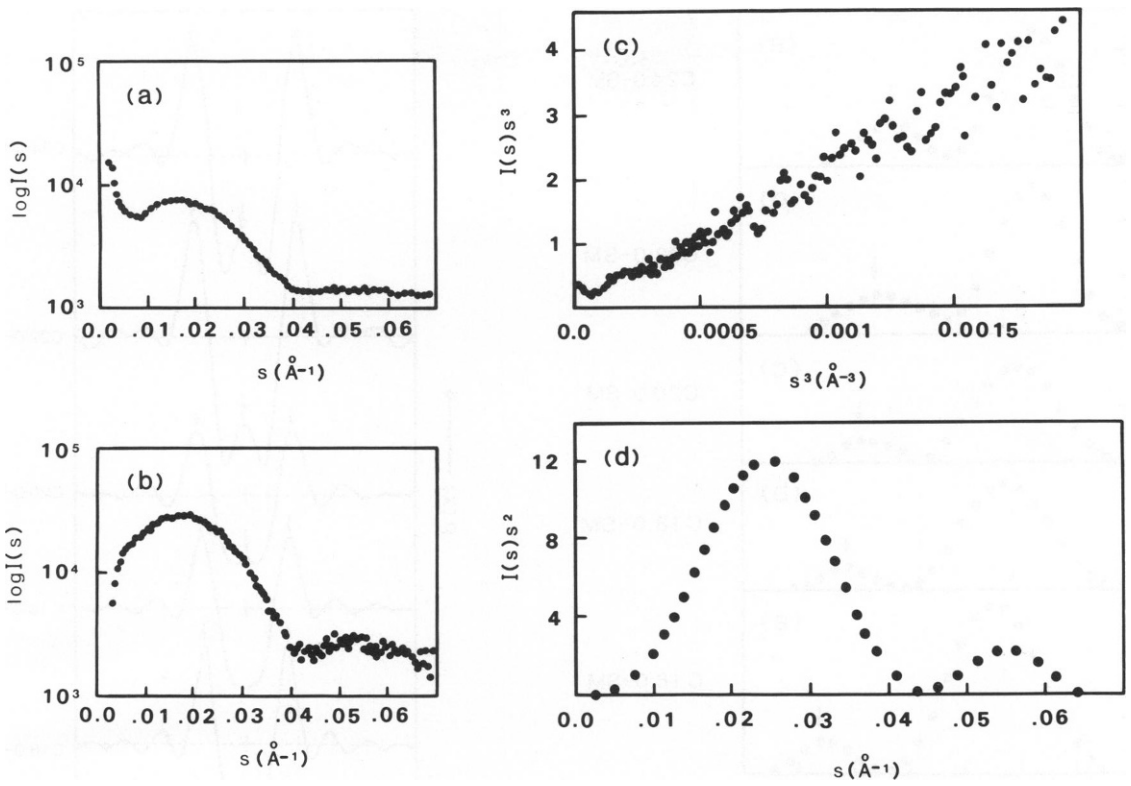

FIGURE 1 (*a*) x-ray scattering intensity (log *I*) as a function of scattering angle ($s = 2 \sin \theta/\lambda$) for single bilayer vesicles of C16:0 SM at 50°C. (*b*) Scattering intensity (log *I*[*s*]) after scaling and buffer subtraction. (*c*) Plot of $I(s)*s^3$ versus s^3 from which the Porod constant *K*2 is obtained. (*d*) Scattering intensity ($I[s]*s^2$) versus *s* following subtraction of *K*2 and Lorentz polarization corrections.

from the Patterson approach. It is recognized that contributions from other parts of the polar group structure contribute to the precise location of the peak maximum in the electron-density profile and, if the polar group extends significantly beyond the phosphate group, that d_{p-p} provides an underestimate of the lipid thickness.

X-Ray Scattering from *N*-Acyl-SM Vesicles

The corrected x-ray scattering curves recorded at 50°C from sonicated vesicles of a series of *N*-acyl-SM varying in chain length from C16:0 to C24:0 are shown in Fig. 3. Two intensity maxima are observed in each case, with the position of both maxima decreasing with increasing chain length. For the weaker second maximum (arrowed), *s* decreases from 0.055 $Å^{-1}$ for C16:0-SM to 0.045 $Å^{-1}$ for C24:0-SM. As described above for C16:0-SM, we have derived the Patterson functions and electron-density profiles by Fourier transformation methods. The Patterson functions for the *N*-acyl-SM are shown in Fig. 4. The arrows indicate the positions of the first prominent, non-origin peak corresponding to the intrabilayer phosphate-phosphate separation (d_{p-p}) in each case. The lipid thickness d_{p-p} increases progressively from 36.5 Å for C16:0-SM to 47.5 Å for C24:0-SM.

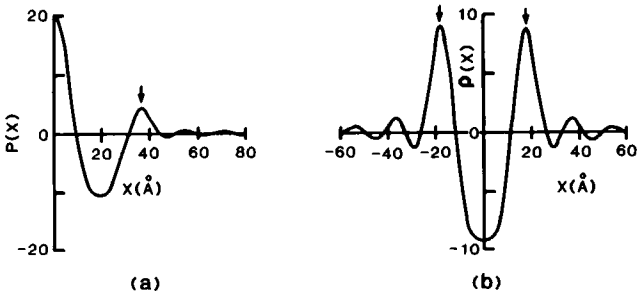

FIGURE 2 (*a*) Patterson function (*P*[*X*]) of C16:0 SM at 50°C following Fourier transformation of $I[s]*s^2$. (*b*) Bilayer electron-density profile ($\rho[X]$) of C16:0 SM at 50°C following Fourier transformation of $\sqrt{(I[s]*s^2)}$.

The corresponding electron-density profiles for the *N*-acyl-SM are shown in Fig. 5. In all cases, two peaks (small arrows) outside a central trough region are observed, with the positions of the maxima increasing from ±18.0 Å for C16:0-SM to ±23.0 Å for C24:0-SM, thus indicating again a progressive increase in bilayer thickness with increasing chain length.

The lipid thicknesses derived using the two approaches are plotted as a function of *N*-acyl chain length in Fig. 6. Both derivations show a linear dependence of d_{p-p} with *N*-acyl chain length and least squares regression lines are shown. From the Patterson data, an increment of 1.40 Å/CH_2 group and an intercept of 14.3 Å are derived. From

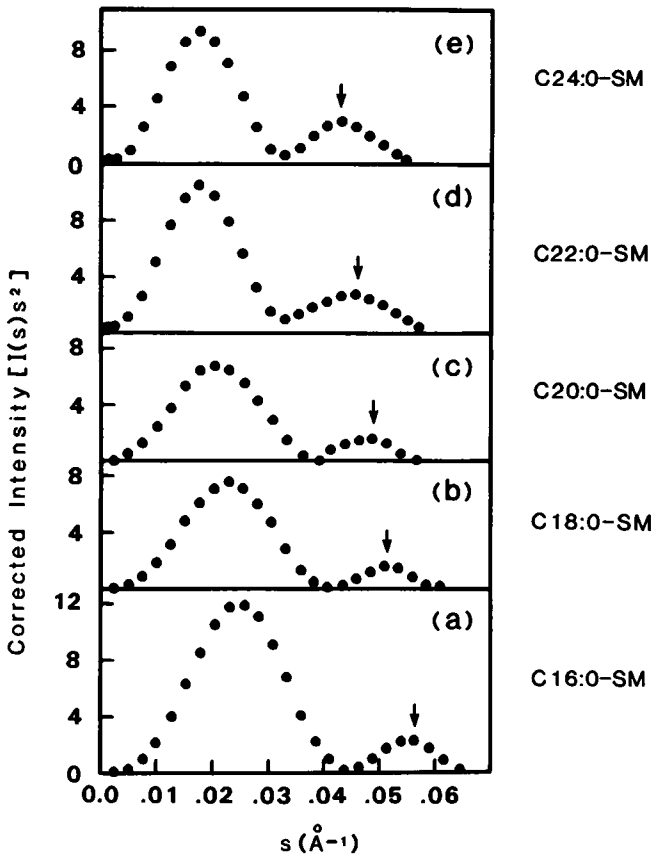

FIGURE 3 Corrected scattering intensity of *N*-acyl SM vesicles at 50°C. (*a*) C16:0 SM, (*b*) C18:0 SM, (*c*) C20:0 SM, (*d*) C22:0 SM, and (*e*) C24:0 SM, calculated as shown for C16:0 SM in Fig. 1. Arrows indicate position of second maximum.

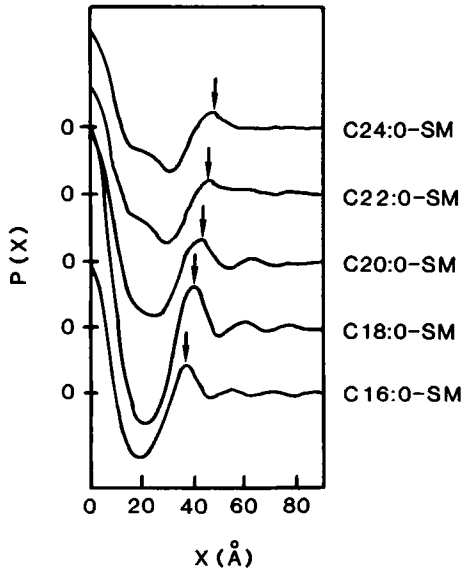

FIGURE 4 Patterson functions ($P[X]$) of C16:0 SM, C18:0 SM, C20:0 SM, C22:0 SM, and C24:0 SM vesicles at 50°C. Arrows indicate positions of first non-origin maximum.

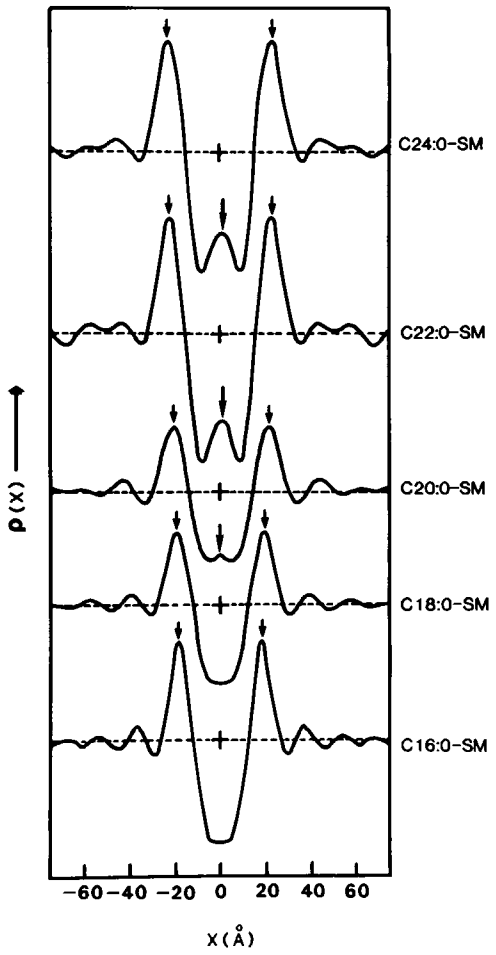

FIGURE 5 Electron density profiles ($\rho[X]$) across the bilayer of C16:0 SM, C18:0 SM, C20:0 SM, C22:0 SM, and C24:0 SM vesicles at 50°C. Small arrows indicate phosphate positions on both sides of the bilayer. Large arrows indicate small maximum in the bilayer center for C20:0 SM, C22:0 SM and C24:0 SM.

the electron-density profiles, an increment of 1.33 Å/CH_2 group and an intercept of 15.0 Å are calculated. These values are in reasonable agreement, small differences being due to (*a*) other contributions in the region of the p − p Patterson vector or (*b*) series termination errors in both Fourier summations, etc. In addition, it should be noted that the shape of the profile at the bilayer center (X = 0 Å; see Fig. 5) is different at different chain lengths. For the shorter chain lengths (C16:0- and C18:0-SM) a simple trough is observed, whereas beginning at C20:0-SM and becoming more pronounced for C22:0- and C24:0-SM, a peak (Fig. 5, large arrows) at the bilayer center is observed. While Fourier termination effects may be contributing, the profiles are suggestive of altered chain packing arrangements in the bilayer center as the *N*-acyl chain begins to differ markedly in length from that of the invariant C18 sphingosine chain of SM.

If the bilayer thickness and partial specific volume ($\bar{v}$) of each SM are known, the molecular area of SM at the lipid-water interface can be calculated. Since no determi-

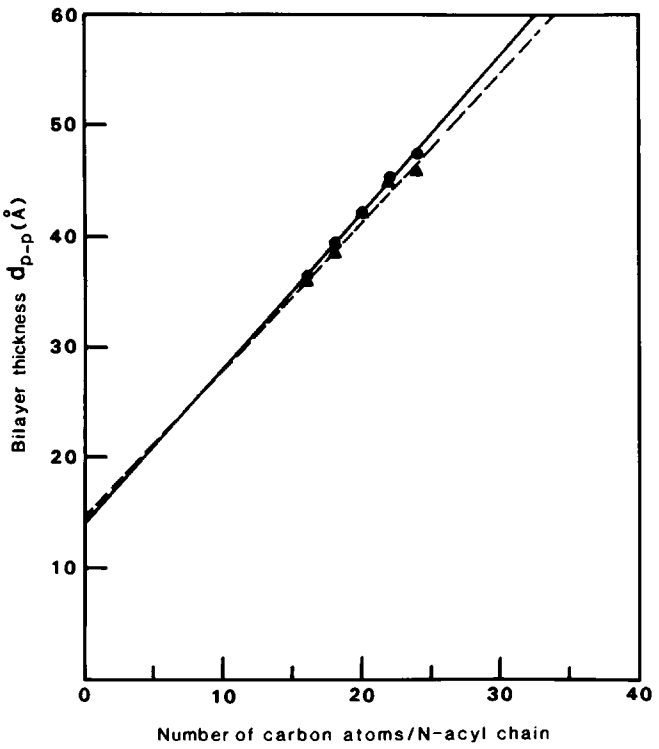

FIGURE 6 Plot of bilayer thickness of *N*-acyl SM vesicles at 50°C: (▲) from electron density profiles, and (●) from Patterson functions.

nations of $\bar{v}$ have been made on SM in vesicles (or multibilayers), we have assumed that the $\bar{v}$ of C16:0-SM is identical to that of di C16:0-PC in multibilayers at 50°C (i.e., $\bar{v} = 1.005$ cm^3/g [15]). From this value of $\bar{v}$, a molecular volume of 1173.1 Å^3 is calculated for C16:0-SM; division by $d_{p-p}/2$ gives a molecular area for C16:0-SM of 64.3 Å^2. Incrementing the molecular volume by 27.7 Å^3 per CH_2 (15), the molecular volumes and surface areas for the *N*-acyl SM series are calculated. As shown in Table I, the area per molecule decreases progressively from a value of 64.3 Å^2 for C16:0-SM to 58.7 Å^2 for C24:0-SM.

DISCUSSION

We have prepared single bilayer vesicles of a series of SM of different chain lengths (C16:0- to C24:0-SM) and used x-ray scattering measurements to derive the bilayer thickness. The measurements have been performed at 50°C, a temperature greater than the chain-melting temperature for all members of the series (9). Thus, the bilayer thickness corresponds to that of the L_α phase. In this state, the bilayer increment is 1.3–1.4 Å/CH_2 group and the intercept 14.3–15.0 Å suggests a contribution of 7–7.5 Å for each SM polar group to the bilayer thickness. It should be clear that if the polar group of SM significantly extends beyond the phosphate group, the actual polar group thickness will be somewhat larger. In a similar study of phosphatidylcholines (4), the Patterson approach was used to measure the bilayer thickness, in this case as both acyl chains were increased in length. For the saturated PC series (di C10:0- to di C16:0-PC) an increment of 1.7 Å/CH_2 group and an intercept of 10.0 Å were obtained (4). The different values of the intercept for the SM and PC series suggests a different conformation at the interfacial sphingosine and glycerol regions in the two cases. On the other hand, the difference in increment observed for the two series is expected, since for the SM series only the *N*-acyl chain is increased (the sphingosine chain is invariant), whereas both *O*-acyl chains are increased for the PC series. For the PC series, the increment is in good agreement with that predicted on theoretical grounds for lipids in the melted-chain L_α state with a significant population of *gauche* chain conformers (16). With only a single chain increasing in the SM series, a simple model in which progessive chain interdigitation occurs (see Fig. 7 *A*) would predict an increment one-half of that observed for the PC series, i.e., ~0.85 Å/CH_2 group. Thus, this simple interdigitation model cannot explain the observed increment of 1.3–1.4 Å/CH_2 group. Clearly, the electron-density profiles of the more asymmetric sphingomyelins, particularly C22:0-SM and C24:0-SM, do show features (peak maxima in the bilayer center, see Fig. 5), the simplest explanation of which is some form of chain overlap or interdigitation. Similar features in the electron-density profiles of gel state interdigitated phospholipid bilayers have been reported previously (17–20). At the other extreme is a model for the SM series showing no interdigitation at the bilayer center (Figure 7 *C*). This model predicts an increment identical to that of the PC series, i.e., ~1.7 Å/CH_2 group. Clearly this model is both inconsistent with the observed increment and energetically unfavorable. Thus, in Fig. 7 *B* we suggest a model at least consistent with the observed increment. For C16:0-SM, the sphingosine and fatty acid chains are approximately equal in length and no chain overlap (i.e., no interdigitation) occurs at the bilayer center. Note also that the bilayer thickness d_{p-p} of di C16:0-PC (4; P. R. Maulik, unpublished observations) is almost identical to that of C16:0-SM (36–37 Å), which suggests that their bilayer structures and chain packing arrangements are similar. For di C16:0-PC, ^{2}H-NMR studies (21) show a low value for the order parameter *S* towards the chain termini, which is indicative of a disordered bilayer center. By analogy, we suggest that a similar degree of chain disorder occurs at the bilayer

TABLE I
SURFACE AREA CALCULATIONS

SM	$\bar{v}$ (calc)	Volume (calc)	$d_{p-p}/2$	S
	cm^3/g	*Å^3*	*Å*	*Å^2*
C16:0	1.005	1173.1	18.25	64.3
C18:0	1.012	1228.5	19.75	62.2
C20:0	1.019	1283.9	21.12	60.8
C22:0	1.025	1339.3	22.75	58.9
C24:0	1.030	1394.7	23.75	58.7

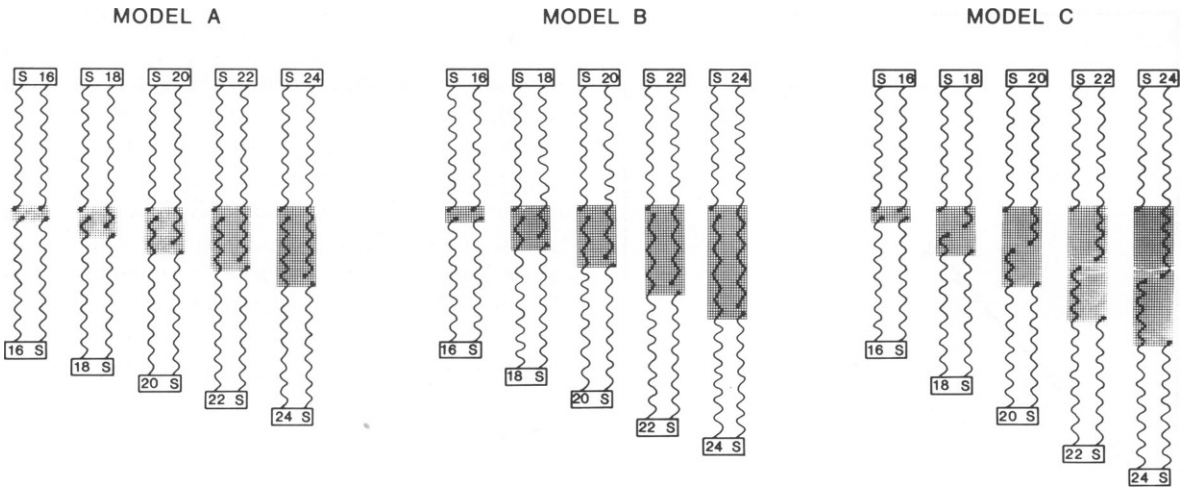

FIGURE 7 Schematic representations of bilayer packing in C16:0-SM to C24:0-SM vesicles. *S* = sphingosine chain. Model A: simple interdigitation model, predicted increment ~0.85 Å/CH_2. Model B: interdigitation accompanied by increased chain order in the interdigitated region (see text), predicted increment ~1.4 Å/CH_2. Model C: non-interdigitated, predicted increment ~1.7 Å/CH_2.

center of C16:0-SM. With increasing chain length for the PC series, similar chain behavior is expected. For the SM series, with increasing fatty acid chain length, progressive interdigitation occurs (see Fig. 7 *B*). However, with increasing chain length, increased chain overlap of fatty acyl chains from opposite sides of the bilayer must occur. We suggest that this chain overlap, coupled to the lack of a well-defined layer of terminal methyl groups, increases the interchain, van der Waals' interactions in the overlap region. This in turn should produce a "more ordered" central region of the bilayer with less *gauche* conformers and a corresponding increase in the C-C-C distance compared to a non-overlapping bilayer. This increase in bilayer order with increased chain length might be expected to result in a progressive decrease in molecular area occupied by SM at the lipid-water interface. Such a decrease is observed (see Table I), although due to the assumptions made in the area calculations these data should be interpreted with caution. This effect is illustrated schematically in Fig. 7 *B* and an increment intermediate between that of models A and C (Fig. 7) is predicted. We are attempting to test this model using higher resolution diffraction studies of C24:0-SM multibilayers in the corresponding melted-chain L_α state as well as ^{2}H-NMR studies of selectively labeled SM (Griffin, R. G., P. K. Sripada, and G. G. Shipley, work in progress).

We thank Dr. P. K. Sripada for synthesis of sphingomyelins, D. Jackson for technical help, and I. Miller for assistance in preparing this manuscript.

This research was supported by research grant HL-26335 and training grant HL-07291 from the National Institutes of Health.

Received for publication 7 April 1986 and in final form 1 July 1986.

REFERENCES

1. Wilkins, M. H. F., A. E. Blaurock, and D. M. Engelman. 1971. Bilayer structure in membranes. *Nature New Biol.* 230:72–76.
2. Chapman, D., D. J. Fluck, S. A. Penkett, and G. G. Shipley. 1968. Physical studies of phospholipids. X. The effect of sonication on aqueous dispersions of egg yolk lecithin. *Biochim. Biophys. Acta.* 163:255–261.
3. Atkinson, D., H. Hauser, G. G. Shipley, and J. M. Stubbs. 1974. Structure and morphology of phosphatidylserine dispersions. *Biochim. Biophys. Acta.* 339:10–29.
4. Lewis, B. A., and D. M. Engelman. 1983. Lipid bilayer thickness varies linearly with acyl chain length in fluid phosphatidylcholine vesicles. *J. Mol. Biol.* 166:211-217.
5. Lewis, B. A., and D. M. Engelman. 1983. Bacteriorhodopsin remains dispersed in fluid phospholipid bilayers over a wide range of bilayer thicknesses. *J. Mol. Biol.* 166:203–210.
6. Calhoun, W. I., and G. G. Shipley. 1979. Fatty acid composition and thermal behavior of natural sphingomyelins. *Biochim. Biophys. Acta.* 555:436–441.
7. Ruocco, M. J., D. Atkinson, D. M. Small, R. P. Skarjune, E. Oldfield, and G. G. Shipley. 1981. X-ray diffraction and calorimetric study of anhydrous and hydrated *N*-palmitoylgalactosylsphingosine(cerebroside). *Biochemistry.* 20:5957–5966.
8. Ruocco, M. J., and G. G. Shipley. 1984. Interaction of cholesterol with galactocerebroside and galactocerebroside-phosphatidylcholine bilayer membranes. *Biophys. J.* 46:695–707.
9. Sripada, P. K., P. R. Maulik, and G. G. Shipley. 1986. Synthesis and properties of a series of N-acyl sphingomyelins. *J. Lipid Res.* submitted.
10. Barenholz, Y., D. Gibbes, B. J. Litman, J. Goll, T. E. Thompson, and F. D. Carlson. 1977. A simple method for the preparation of homogeneous phospholipid vesicles. *Biochemistry.* 16:2806–2810.
11. Bartlett, G. R. 1959. Phosphorus assay in column chromatography. *J. Biol. Chem.* 234:466–468.
12. Muller, K. 1982. Experimental practice. *In* Small Angle X-Ray Scattering. O. Glatter and O. Kratky, editors. Academic Press, London. 215–236.
13. Yeager, M. J. 1976. Neutron diffraction analysis of the structure of retinal photoreceptor membranes and rhodopsin. *In* Neutron Scattering for the Analysis of Biological Structures. B. P. Schoenborn, editor. Brookhaven National Laboratory, New York. III-3–36.
14. Laggner, P., A. M. Gotto, Jr., and J. D. Morrisett. 1979. Structure of the dimyristoylphosphatidylcholine vesicle and the complex formed by its interaction with apolipoprotein C-III: X-ray small-angle scattering studies. *Biochemistry.* 18:164–171.

15. Nagle, J. F., and D. A. Wilkinson. 1978. Lecithin bilayers. Density measurements and molecular interactions. *Biophys. J.* 23:159–175.
16. Marcelja, S. 1974. Chain ordering in liquid crystals. II. Structure of bilayer membranes. *Biochim. Biophys. Acta.* 367:165–176.
17. Ranck, J. L., T. Keira, and V. Luzzati. 1977. A novel packing of the hydrocarbon chains in lipids. The low temperature phases of dipalmitoyl phosphatidyl-glycerol. *Biochim. Biophys. Acta.* 488:432–441.
18. McDaniel, R. V., T. J. McIntosh, and S. A. Simon. 1983. Nonelectrolyte substitution for water in phosphatidylcholine bilayers. *Biochim. Biophys. Acta.* 731:97–108.
19. Serrallach, E. N., R. Dijkman, G. H. de Haas, and G. G. Shipley. 1983. Structure and thermotropic properties of 1,3-dipalmitoyl-glycero-2-phosphocholine. *J. Mol. Biol.* 170:155–174.
20. Mattai, J., and G. G. Shipley. 1986. The kinetics of formation and structure of the low temperature phase of 1-stearoyl-lysophosphatidylcholine. *Biochim. Biophys. Acta.* 859:257–265.
21. Seelig, J., and A. Seelig. 1980. Lipid conformation in model membranes and biological membranes. *Q. Rev. Biophys.* 13:19–61.